CHAPTER ONE HUNDRED NINETEEN

Suspended Sand Transport on a Dissipative Beach

John P. Downing*

ABSTRACT

Field studies were conducted in November 1979 to measure suspended sand transport on Twin Harbor Beach, Washington U.S.A. This beach has an average slope of 0.02 and is composed of well-sorted sand with a mean diameter of 0.21mm. The significant height of breaking swells approaching the beach at small angles can be estimated from variance spectra of water level by $4.36\,\sigma_\eta$. In the surf zone significant wave heights are linearly related to the local mean water depth by $\gamma = H_s/h \approx 0.45$. Variance, σ^2_n, in the gravity wave band (0.048 to 1.0 Hz) is proportional to water depth squared. Low-frequency variance (less than 0.048 Hz) although not systematically related to water depth, is usually largest in the inner surf zone where breakers are small.

Sand suspension is correlated with strong offshore flows that recur at about one-fifth the incident wave frequency. Vertical mixing of sand in the water column by these water motions rather than turbulence generated by shear at the bed associated with individual wave oscillations is a key mechanism in sand transport on dissipative beaches.

The largest sediment loads occur in the inner surf zone where low-frequency motions dominate the breakers. Maximum longshore transport rates, however, were measured in the middle of the surf zone because of the higher longshore current speeds there. The suspended load probably accounts for as much as 45 percent of the litoral drift on a dissipative beach exposed to moderately-high swells approaching the shore at small angles.

INTRODUCTION

Sand transport by shoaling waves and nearshore currents in the surf zone is a key process controlling the plan and profile of sandy shores. Nearshore circulation and sand transport vary from one coastal area to another depending upon beach morphology, sediment size, and wave climate. These variations form a continuum of surf dynamics between steep reflective beach systems and gently-sloped dissipative ones. Reflective beaches have narrow surf zones with plunging and collapsing breakers whereas dissipative beaches have wide surf zones with spilling breakers, low frequency current and water level oscillations, and bar-trough morphologies. Several intermediate states of surf dynamics have been scaled with a parameter:

$$\varepsilon = A_1 \omega_1^2 / g \tan^2 \beta \qquad (1)$$

* Northern Technical Services, Inc., 14715 N.E. 95th St., Redmond, WA 98052. Formerly: School of Oceanography, University of Washington

(1, 6, 19, 20 and 21) where: A_i = breaker amplitude, ω_i = incident wave radial frequency; g = gravitational acceleration, and tan β = beach slope. Dissipative beaches are in the range $33 < \varepsilon < \sim 400$ (20).

The Nearshore Sediment Transport Study (NSTS), begun in 1977, was designed to expand the data base on nearshore sediment dynamics for engineers and coastal managers. As part of NSTS an instrumentation system consisting of: 1) an array of optoelectronic sensors, 2) an electromagnetic current meter, 3) a resistance wave gauge, and 4) a portable data acquisition system was installed on Twin Harbors Beach, Washington U.S.A. (4) in November 1979. Water level, current and sediment concentration data were acquired to characterize the fields of suspended sand and horizontal water motions across a dissipative open-ocean beach.

SITE DESCRIPTION

Twin Harbors Beach is on the exposed part of a large barrier spit that forms the seaward margin of Grays Harbor, (Figure 1). The coastline follows a beach ridge complex formed by rapid marine and eolian accretion in the past 5,000 years (2).

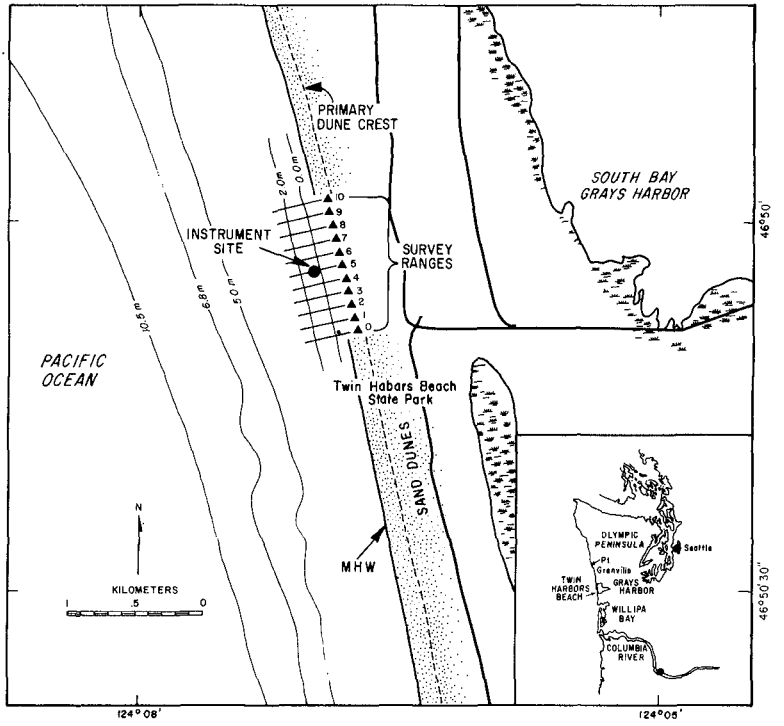

Figure 1 Twin Harbors Beach location map and bathymetry of the study area.

The nearshore bathymetry at the experiment site was determined from 14 rod and level surveys conducted between January and November 1979 along the rangelines shown on Figure 1. The beach is divisible into three zones. The upper beach face has no berm and is relatively steep, $0.06 < \tan \beta < 0.15$. In the zone between 25 and 200 m, the profile is featureless and concave up with constant slope (0.01-0.03); see Figure 2. Mean beach slope is irregular seaward of about 200 m because longshore bars and troughs form there during storms. Fluctuations in beach elevation, during the survey period were largest in the outer zone, where 2.0 m fluctuations were measured. Sand level fluctuations landward ranged from 0.2 to 0.3m during the year.

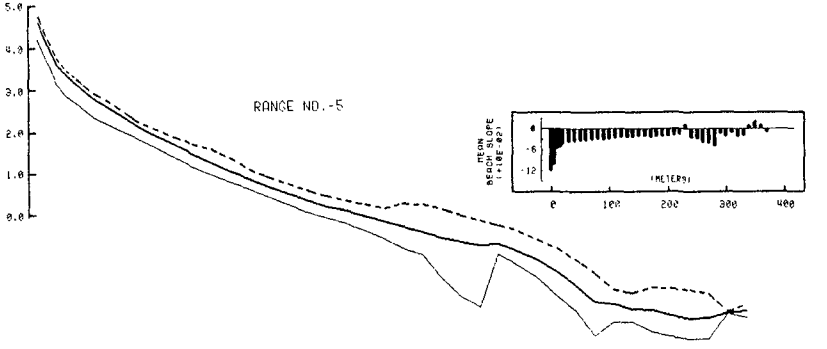

Figure 2 Mean beach profile at range 5 January through November 1979.

The mean grain size and sorting coefficient of sand at the experiment site are 0.21 mm (2.22 Phi) and 0.05 mm (0.38 Phi), respectively (15).

Twin Harbors Beach is exposed to the swell and wind wave regime of the northeast Pacific. The net longshore transport rate near the site estimated by the U.S. Army Corps of Engineers (18), is 2.2×10^6 cubic yards per year to the north. This exceeds the net transport rates on all California and east coast beaches for which historical data exist by a factor of 2 to 4 (17). In accordance with the scheme applied to exposed Australian beaches by Wright et al. (19), Twin Harbors Beach has a very dissipative surf zone with ϵ values between 80 and 240.

INSTRUMENTATION

Figure 3 shows the instrumented mast used for this investigation. Detailed descriptions of individual sensors are given by Downing in (3 and 4). Water level was determined with a surface piercing resistance wave sensor; horizontal current velocity was measured with a MARSH-McBIRNEY electromagnetic current meter and suspended sand concentrations were detected with an integrating infrared back-scatterometer. Analog voltage signals from these sensors were sampled at the rate of 10 H_z, digitized with 12-bit resolution, and recorded on floppy disks with a portable data acquisition system. Twelve-bit digitization produces nominal resolution of one part in 4096 for each measured parameter.

The sensor array was installed on survey range no. 5, 180 m from benchmark-BM 5 (Figure 4). The sensors were mounted on a rigid mast held in place by three guy wires attached to anchor stakes driven into the beach sand. The vertical positions of the sensors were measured relative to the sea bed at the instrument mast. The orientation of the current meter probe was established with a magnetic compass and spirit level and is accurate to $\pm 2^{o}$ of azimuth and $\pm 0.5^{o}$ relative to vertical. The X axis of the probe was aligned with the local isobaths as determined by the beach surveys. Table 1 lists the vertical positions of the sensors with respect to the beach face.

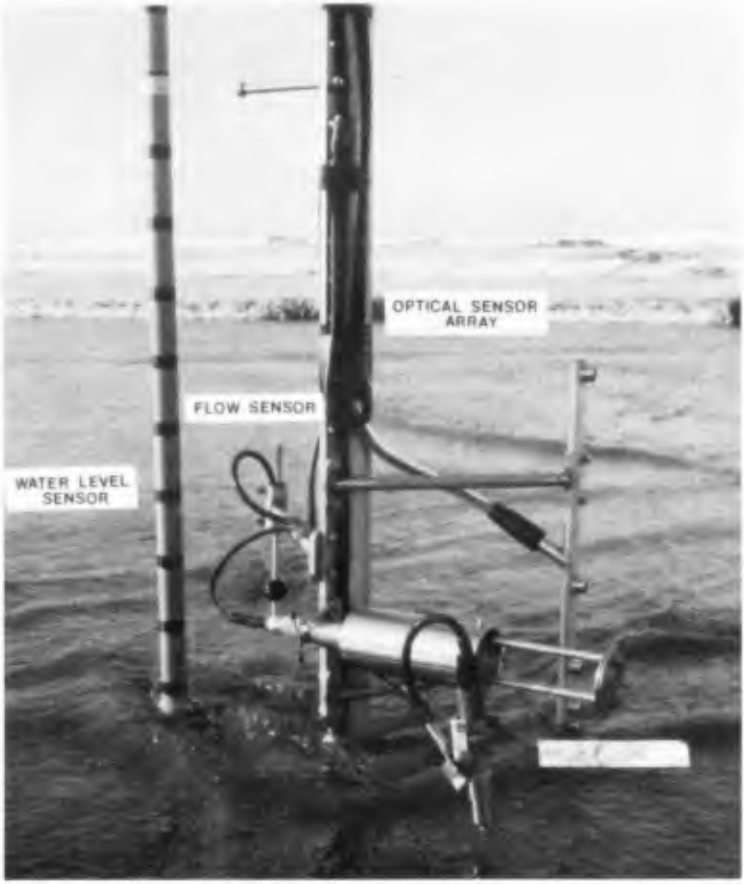

Figure 3 Sediment transport instrument installation.

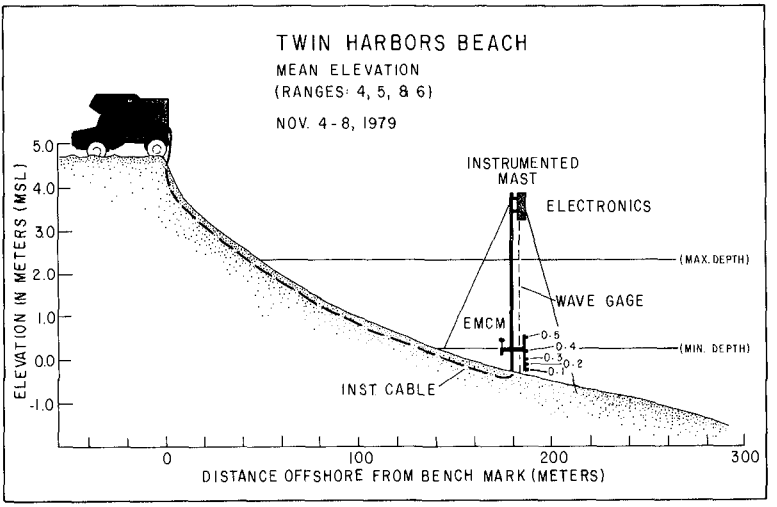

Figure 4 Location of instrumentation on range No. 5.

Table 1. Sensor Locations.

Sensor	Range	Parameter	x (m)	z (m)
EMCM	5	U V	180.2	0.18
Water Level	5	h	180.0	0-3.5
OBS-1	5	C_s	180.2	0.025
OBS-2	5	C_s	180.2	0.055
OBS-3	5	C_s	180.2	0.115
OBS-4	5	C_s	180.2	0.235
OBS-5	5	C_s	180.2	0.535

Notes:

x = Distance offshore from survey baseline.
z = Elevation above sea bed.
U = Alongshore velocity.
V = Shore-normal velocity.
h = Water Depth.
C_s = Suspended sand concentration.

DATA PROCESSING

The coordinate system for computations consists of an X axis, positive onshore; an alongshore Y axis, positive to the north; and a Z axis which is positive up. The origin of the Z axis is the bed elevation at the instrumentation mast.

The binary data were block-averaged over a 0.4-second time window to reduce the bandwidth from 5.0 to 1.25 Hz. The block-averaged time series of (t), U and V(t), and $C_s(t)$ were Fourier transformed using a

Cooley-Tukey algorithm to determine the distribution of variance with frequency. Prior to the transformation, records of 1024 points were demeaned, linearly detrended, and tapered with a cosine window. The raw spectral estimates of four sequential non-overlapping records were ensemble averaged and then smoothed by averaging over a four point spectral window. The resulting spectral estimates have 32 degrees of freedom and represent the mean variance in a bandwidth of 0.0098 Hz.

For the purpose of comparing wave heights across the surf zone, a statistic, H_s, called the significant breaker height was computed from the spectral density functions (SDF), $S_\eta(f)$, for each record. This statistic represents $4\sigma_\eta$ (σ_η equals the square root of the variance) in the frequency band from 0.047 to 1.25 Hz. The variance in this frequency band was computed from the SDFs of $\eta(t)$ by summing the estimates, $S_\eta(fn)$, from n = 20 to 512:

$$\sigma_\eta^2 = \sum_{n=20}^{512} S_\eta(f_n) \tag{2}$$

This is equivalent to computing σ_n from a band-passed record of $\eta(t)$.

Conversions of voltage levels to scientific units were made with the instrument gains and offsets determined from laboratory calibrations made before and after the experiment (4). Computations of instantaneous suspended sand flux in kg/m/s were made by evaluating the integrals:

$$Q_x(t) = U(t)\int_o^h C_s(z,t)\, dz \tag{3}$$

$$Q_y(t) = V(t)\int_o^h C_s(z,t)\, dz \tag{4}$$

where the units of C_s are mass per unit volume and h is the instantaneous water depth.

Several assumptions were made to simplify these computations. First, it was assumed that sand concentration varied linearly between sensors. At the bed, the concentration was estimated by extrapolating the gradient between the lowest two sensors to the bottom. C_s at the surface was set equal to zero. This assumption results in under estimation of the suspended load since the vertical gradients are exponential. It was further assumed that horizontal velocity was vertically uniform. As will become clear later, this assumption was not valid when applied to the computations of shore-normal transport rates. The assumption was unavoidable, however, because only one current meter was deployed.

RESULTS

Wave, current and suspended sand data were acquired during five periods (runs) on the 6th, 7th and 8th of November, 1979. The duration of runs ranged from 1 to 3.5 hrs. and with the exception of Run no. 4, all were completed during ebbing tides.

The surf during this period originated from a large low-pressure disturbance that occurred in the Northeast Pacific Ocean between the 2nd and 4th of November. Sustained winds of 40 knots blew over a fetch more than 4,000 miles long during the most intense part of the storm. Twelve to fifteen second swells began to break on Twin Harbors Beach during the afternoon of November 4th and continued to produce a moderate surf until the afternoon of November 7th.

Wave Conditions

The results of spectral analyses of the water level records are summarized in Table 2 which gives the frequencies and corresponding periods of maxima and minima of the smoothed SDFs. Examples of time series of water level and SDFs representative of conditions in the outer, middle, and inner surf zone are shown in Figures 5 and 6. Spectral density decreases with frequency as f^{-3} to $-7/3$ and the primary spectral peak is between 0.0093 and 0.0267 Hz (37.5 and 107 s). A secondary peak associated with the incident swell occurs between 0.067 and 0.105 Hz (9.5 and 15 s). Periods associated with these spectral peaks averaged over all the records are 13.3 and 67 seconds.

Minima are consistently present in the SDFs of (t) at about 0.048 Hz (T = 21.5 s). This is considered to be the low frequency limit of free surface and velocity fluctuations associated with the incident waves. Water motions and free surface oscillations with frequencies less than 0.047 Hz are called low frequency oscillations. The maximum significant wave height of 1.0 m was measured during the first part of Run no. 2 in a mean water depth of 2.17 m and a corresponding offshore distance of 114 m. About half of the waves early in Run no. 2 were unbroken and the offshore distance of 114 m is taken as the width of the surf zone (x_b) during the experiment. Wave heights are linearly proportional water depth and ranged from 0.21 m at $x/x_b = 0.35$ to 1.0 m at $x/x_b = 1.0$.

Currents

The longshore current, during 94 percent of the experiment was towards the south with an average speed 0.27 m/s. During two 13.7 min periods it reversed direction and flowed to the north usually less than 0.01 m/s. The maximum 6.83-minute average longshore current was 0.66 m/s.

The persistent southly longshore current indicates that waves approached the beach from the northwest throughout the experiment and that cellular circulation, rip currents, and large horizontal eddies did not occur during most of the study. Shore-normal current components were offshore during all runs with mean and maximum speeds 0.15 and 0.37 m/s respectively. The implications of a net offshore flow are discussed in a later section.

Suspended Sand Concentrations and Transport

Measured transport rates varied between 0.01 and 1.00 Kg/m/s during the experiments and are representative of offshore distances ranging from X = 0.35-1.0. Figure 6 shows time series of sand concentrations in

the water column at three locations across the surf zone. Sand suspension on this beach is a transient phenomena which occurs at time intervals much longer than the period of the incident waves. The duration and number of sand suspension events increases with decreasing water depth, and they are associated with prolonged periods of offshore flow.

The vertical distribution of suspended sand in the water column has two distinct forms. During quiescent intervals between suspension events, the water column is lightly charged with sediment and the concentration of sand is vertically uniform; see Figure 7. During suspension events, when large quantities of sand are mixed in the water column, there is a strong concentration gradient to about 10 cm above the bed. Above this level sand concentration is more vertically uniform.

Table 2 Summary of time-averaged water level, current and sand transport data.

Run No.	Date	(Time)	$\bar{X}$	$\bar{h}$ (m)	$\bar{T}_1$ (s)	$\bar{H}_s$ (m)	$\bar{T}_w$ (s)	$\bar{U}$ (m/s)	$\bar{V}$ (m/s)	M (kg/m^2)	$\bar{Q}_x$ (kg/m.s)	$\bar{Q}_y$ (kg/m.s)
1	6-Nov.	(01:53)	.82	1.65	93.8	.72	13.2	-.20	-.44	.336	-.071	-.159
1	6-Nov.	(02:21)	.81	1.58	75.0	.65	13.2	-.20	-.56	.508	-.138	-.266
1	6-Nov.	(02:48)	.76	1.46	53.6	.63	12.9	-.18	-.46	.398	-.045	-.191
1	6-Nov.	(03:16)	.69	1.25	85.0	.55	13.3	-.19	-.31	.639	-.067	-.251
1	6-Nov.	(04:04)	.55	.88	78.8	.42	15.0	-.24	-.31	2.074	-.995	-.561
RUN MEANS			.73	1.36	76.4	.59	13.9	-.20	-.42	.791	-.263	-.286
2	6-Nov.	(13:06)	.98	2.15	50.0	1.04	13.2	-.28	-.38	.271	-.074	-.117
2	6-Nov.	(13:33)	.95	2.05	75.2	.93	12.9	-.17	-.41	.211	-.028	-.088
2	6-Nov.	(14:01)	.90	1.89	75.2	.83	12.9	-.20	-.38	.176	-.028	-.069
2	6-Nov.	(14:28)	.84	1.69	50.0	.72	12.9	-.18	-.09	.124	-.017	-.013
2	6-Nov.	(14:55)	.75	1.42	56.7	.60	13.0	-.17	-.04	.113	-.013	-.005
RUN MEANS			.88	1.84	64.0	.82	13.0	-.20	-.26	.179	-.032	-.058
3	7-Nov.	(01:56)	.80	1.58	50.0	.73	11.7	-.13	-.27	.250	-.026	-.066
3	7-Nov.	(02:23)	.80	1.57	83.3	.70	11.5	-.10	-.25	.166	-.011	-.037
3	7-Nov.	(02:51)	.47	.70	52.7	.47	12.9	-.16	-.05	8.508	-.715	-.282
RUN MEANS			.69	1.28	59.2	.63	12.3	-.13	-.19	2.975	-.251	-.128
4	7-Nov.	(12:40)	.86	1.74	37.5	.79	12.7	-.12	-.30	.090	-.006	-.027
4	7-Nov.	(13:07)	.88	1.84	50.0	.84	10.3	-.09	-.28	.074	-.006	-.021
4	7-Nov.	(13:35)	.90	1.87	53.0	.86	15.1	-.13	-.23	.069	-.012	-.160
RUN MEANS			.88	1.82	46.8	.83	12.7	-.11	-.27	.078	-.008	-.069
5	8-Nov.	(05:47)	.82	.82	50.0	.39	13.2	-.05	-.25	.423	-.020	-.106
5	8-Nov.	(06:14)	.66	.66	93.8	.32	NS	-.08	-.04	.502	-.028	-.010
5	8-Nov.	(06:42)	.50	.55	107.0	.23	NS	-.07	-.09	.865	-.012	-.051
5	8-Nov.	(07:09)	.39	.39	50.0	.19	11.8	-.06	-.04	1.900	-.134	-.030
RUN MEANS			.59	.61	75.2	.28	12.5	-.07	-.11	.923	-.049	-.049
GRAND MEANS			.75	1.38	64.3	.63	12.9	-.14	-.25	.989	-.121	-.118

Notes:

NS Not significant.

$X = x/x_b$

x_b = width of surf zone)

T_1 = Period of spectral density peaks.

T_w = Period of spectral density peak associated with incident waves.

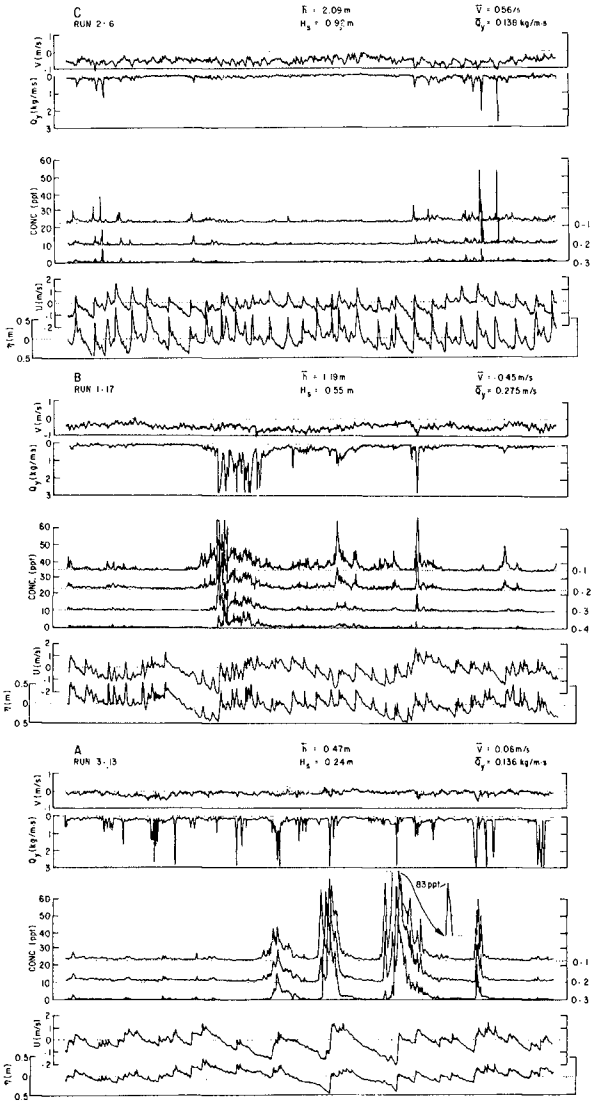

Figure 5 Time series of water level, currents, suspended sand concentrations, and longshore sand transport in the A) inner, B) middle, and C) outer surf zone.

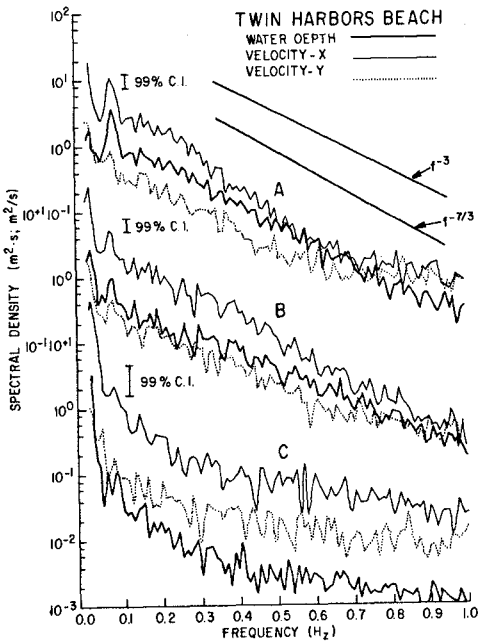

Figure 6 Wave and current spectra for A) outer, B) middle, and C) inner surf zone.

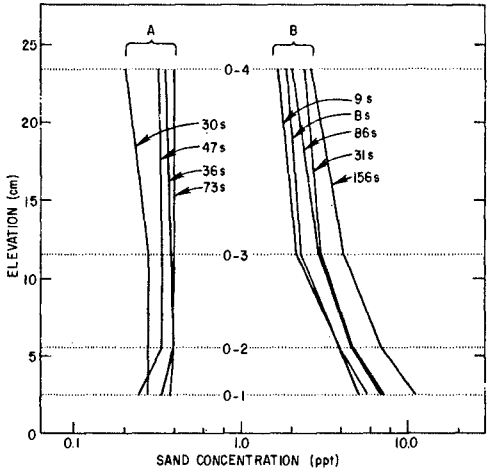

Figure 7 Suspended sand concentration profiles
A. During quiescent conditions
B. During suspension events
Profile annotations indicate the averaging time in seconds.

DISCUSSION

The variance spectrum of water level is convenient to compute, and an empirical check was made to determine how closely measured significant breaker heights can be approximated from the total variance in the gravity wave band. Measurements of the crest to trough heights of 434 spilling breakers across the surf zone indicate that H_s is best approximated by $4.36\,\sigma_\eta$. This approximation is probably site specific but indicates that a useful wave height parameter can be easily computed from the variance spectrum.

The variation of H_s with local depth is linear, and the breaking criteria, γ, is 0.45 ± 0.05. Because several formulas for computing orbital velocities, setup and runup, include the "constant," γ; a comparison of field-determined breaking criteria is given in Table 3. These data indicate that γ varies with beach and surf conditions and should be selected cautiously.

Table 3. Wave breaking criteria.

Beach Slope ($\tan\beta$)	γ	Beach	Reference
0.011	0.42	Goolwa, Aust.	(20)
0.014	0.6	Saunton, G.B.	(7)
0.02	$0.45 \pm .05$	Twin Harbor Beach, WA	This study
0.13	1.2	Slapton, G.B.	(7)

In Figure 9 computed values of wave energy, E_w, and total energy, E_T, have been plotted versus water depth to illustrate possible wave energy decay processes. A least squares fit is drawn through the E_w values to indicate the trend of wave decay. The distance between this curve and the plotted values of E_t provides an estimate of the energy associated with low frequency motions. A gradient of wave energy is developed across the surf zone and dissipation is manifested in the growth of low frequency oscillations in water level with attendant fluctuations in the shore-normal current. The energy transfer from high to low frequency, revealed by the present analysis, is not systematic. There is considerable variability in low-frequency energy across the surf zone which cannot be characterized by a convenient parameter such as H_s. High values of total energy are more likely in the outer surf zone but are not restricted there. Peak values appear at regularly spaced intervals across the surf zone suggesting a standing wave with antinodes at h = 0.80 m and h = 1.60 m (X = 0.53 and 0.82).

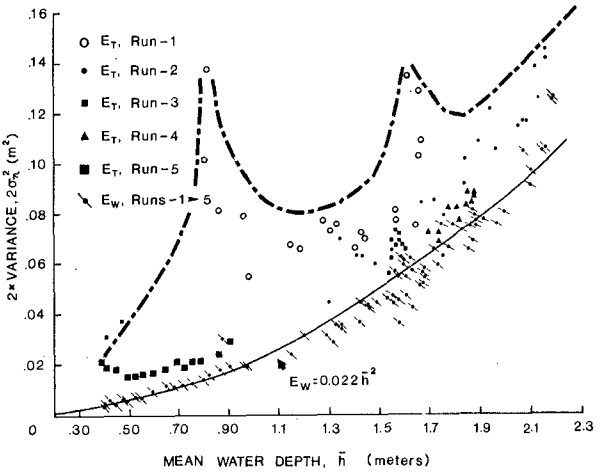

Figure 8 Graph of wave energy, E_w, and total energy, E_t, versus water depth.

The mean shore-normal velocity component at Z = 18 cm is 0.15 m/s offshore. Offshore flow at mid-depth is predicted by some theories and laboratory experiments (12 and 16), but is not consistent with most other field data (6) except that from Goolwa Beach, Australia (20). It appears that the mass transport under shoaling waves on highly dissipative beaches can be balanced by nearshore circulation other than eddies and rip currents (10). The total loss of sand from the beach on a weekly basis computed from the profile data (5 to 8 November) was only 0.06 m^3. This is nearly three orders of magnitude less than the sand loss of 50 m^3 per week calculated from the shore-normal transport data, a large discrepancy. In order to balance the sand budget, it appears there must be onshore sand transport near the bed since there is rarely enough suspended sand above z = 18 cm to balance the loss at mid-depth. This result underscores the importance of measuring velocities at several elevations, especially nearer the bed, when monitoring total transport.

Variation of Sand Transport and the Total Load

The changing character of the wave induced water motions and sand suspension across the surf zone, Figure 5, and their effect on longshore sand transport is more evident when time and space averaging of the currents and suspended load is done. The 6.8-minute average values of V, M and Q_y for all runs were grouped according to their location across the surf zone into bins 10 meters wide. Average values for these parameters in each of the bins were normalized by their respective maxima, and their variation across the surf zone is shown on Figure 9.

In the mid- to outer surf zone, x = 75-115 m, the longshore current is large and decreases linearly to 1/10 of the maximum value in the inner surf zone. The suspended sand load is uniformly low in the outer surf zone, x = 85-115 m, and increases near shore. Longshore sand flux is low in the outer zone, primarily because there is little suspended sand available for transport by the high currents there. Q_y peaks in the mid- to inner zone where the suspended load is moderately high and longshore current speeds are nearly maximum. Near shore the sediment load reaches a maximum but the longshore current is minimal, producing only moderate transport. This general trend of high longshore transport in the mid-surf zone with decreased rates both on and offshore supports Komar's (9) model for the total longshore transport.

Komar (9 and 10) has reviewed the energetics approach to sand transport prediction and indicates that equation 4 represents the longshore transport resulting from radiation stresses as well as nearshore currents from the tides and winds. The total longshore transport is given by:

$$Q_s = 2.5\ (EC_n)_b \frac{\overline{V}_l}{U_m} \tag{4}$$

where Q_s is the at-rest volume of sand transported per day (m^3/day); EC_n is the wave energy flux at the breaker zone; $\overline{V}_l$ is the mean longshore current in the middle of the surf zone and U_m is maximum orbital velocity under the breakers. The advantage of this equation is that breaker angles which are difficult to measure do not appear explicitly. Maximum orbital velocity is given by (10):

$$U_m = \gamma/2\ [g\ (\bar{\eta} + h)]^{1/2} \tag{5}$$

A comparison of total measured advective sand transport with total predicted longshore transport was made to estimate the contribution of the suspended load. The total transport estimate is made with the wave conditions observed during the early part of Run no. 2, since the instrument was located in the zone of initial wave breaking. The quantity $(\bar{\eta} + h)$ is replaced by the measured mean water depth $\bar{h}$ which includes setup $\bar{\eta}$, and the breaking parameter, γ, is taken as 0.7 times the measured value since RMS wave heights are used in Komar's formula. Likewise the wave energy flux is computed with

$H_{rms} = 0.7\ H_s$; so $EC_n = \frac{1}{8}\ \rho g\ H_{rms}^2 \sqrt{gh}$. The longshore current velocity

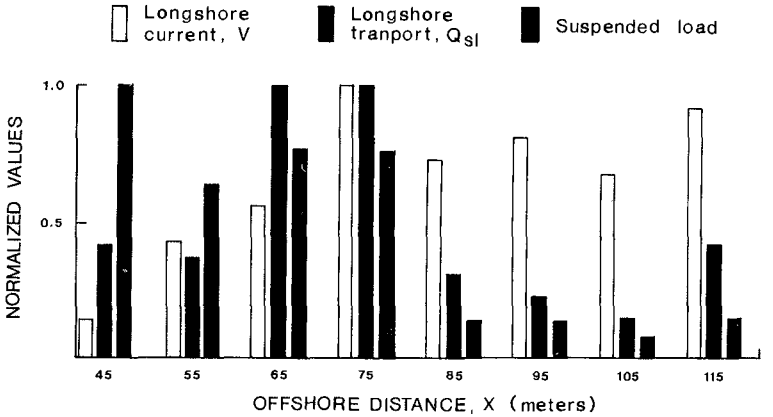

Figure 9 Variation of longshore current speed, suspended load, and sand transport across the surf zone.

at the mid-surf position is given by the average of the longshore velocities measured in water depths between 0.7 and 1.0 m. The values used for computing Q_s are: H_{rms} = 0.59 m; $\bar{h}$ = 2.1 m; $\bar{V}_l$ = 0.25 m/s and U_m = 0.64 m/s. The predicted total longshore transport rate is 1,930 m^3/day.

In making the estimate of advective sand transport, the surf zone was subdivided into twelve shore-parallel bands, 10 meters wide. Transport rates in each band are equal to the average of measured values in the band. Values in the inner surf zone are obtained by linear extrapolation of the innermost measurements to zero at the shoreline. In this way, a value of 915 m^3/day was estimated for the suspended load transport during the experiment. This comprises 47 percent of the total load predicted above.

Wave-sediment Interaction

Suspension events appear to be the major process which makes sand available for advective transport on Twin Harbors Beach. More than 190 suspension events were recorded during the ten hours of measurements. These events nearly always occurred during offshore flow that persists for several wave periods (Figure 6). Three of these events have been selected for description and are illustrated in Figure 10.

For each event, the time histories of sand concentration at the lowest four sensors and horizontal current speed are shown with a sequence of C_s profiles. The suspension events occur as follows:

1) The water column is relatively clear during initial offshore acceleration of the flow.

2) High concentrations and gradients develop near the bed and sand is mixed into the water column as bores propagating shoreward interact with the seaward flowing current. There is usually a lag of several seconds between the occurrence of high sand concentrations near the bed

and their occurrence in the upper water column (z > 24 cm). Maximum sediment loads usually lag peak offshore current speeds and the passage of the larger bores.

3) The decay of suspension events is most often characterized by a loss of suapended load with a uniform decrease of concentration at all levels.

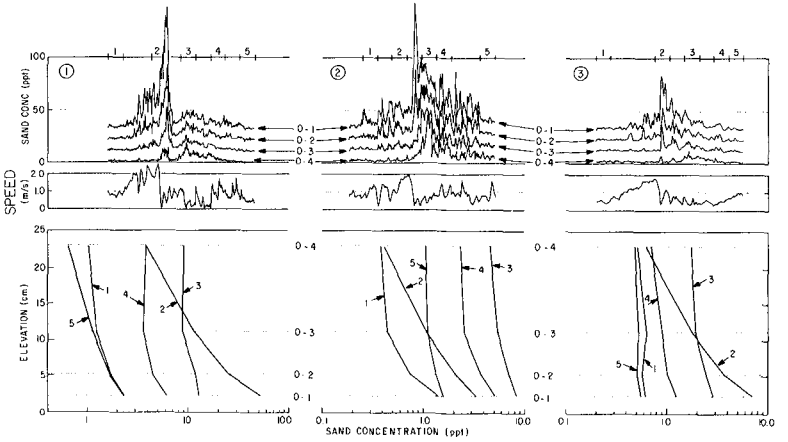

Figure 10 Sequential suspended sand profiles during suspension events. Numbered intervals on upper axis are six seconds long; current speeds are the resultant of X and Y-velocity components. Concentration profiles are six-second averages.

Several important aspects of the water motion producing these suspension events could not be measured for the present study. These include the vertical velocity component and the local convective accelerations. These respects of water motion appear to be critical to our full understanding of the suspension process (8). Further it appears that the approach to the problem of suspended sand transport taken in previous investigations (11 and 13) may not be productive on natural dissipative benches since wave by wave sand suspensions are a small part of the total load.

CONCLUSIONS

At Twin Harbors Beach:

1) The significant height of breaking swells approaching the beach at small angles can be estimated from variance spectra of water level by $4.36\sigma_\eta$. In the surf zone significant wave heights are linearly related to the local mean water depth by $\gamma = H_a/h = 0.45$. Variance, σ_η^2, in the gravity wave band (0.048 to 1.0 Hz) is proportional to water depth squared. Low-frequency variance (less than 0.048 Hz) although not systematically related to water depth, is usually largest in the inner surf zone where breakers are small.

2) Sand suspension is correlated with strong offshore flows that recur at about one-fifth the incident wave frequency. Vertical mixing of sand in the water column by these water motions rather than turbulence generated by shear at the bed associated with individual wave oscillations is a key mechanism in sand transport on dissipative beaches.

3) The largest sediment loads occur in the inner surf zone where low-frequency motions dominate the breakers. Maximum longshore transport rates, however, were measured in the middle of the surf zone because of the higher longshore current speeds there. The suspended load probably accounts for as much as 45 percent of the littoral drift on a dissipative beach exposed to moderately-high swells approaching the shore at small angles.

ACKNOWLEDGMENTS

I thank Professors Dick Sternberg and Clive Lister for their insight and productive suggestions about this research. Rex Johnson and Stan Woods were the skilled craftsmen who made the instruments. Harvey Smith provided energetic support in the field. Financial support was provided by a NOAA grant administered by the National Sea Grant College Program and the Nearshore Sediment Transport Study, a milti-institutional effort (#SGNOAA NA8I KA-D-0030).

REFERENCES

1. Battjes, J. 1975. Surf similarity. Proc. 14th Coastal Eng. Conf., ASCE, pp. 466-479.

2. Cooper, W. S. 1958. Coastal sand dunes of Washington and Oregon. Geol. Soc. Amer. Memoir 72, 169 p.

3. Downing, J. P., R. W. Sternberg and C. R. B. Lister. 1981. New Instrumentation for the Investigation of Sediment Suspension Processes in the Shallow Marine Environment. In Nittrauer, C. A. (ed.), Sedimentary Dynamics of Continental Shelves: 19-34. Mar. Geol. 42 (Special Issue).

4. Downing J. P. 1983. Field Studies of Suspended Sand Transport, Twin Harbor Beach, Washington. Ph.D. Dissertation, University of Washington, Seattle, Washington.

5. Guza, R. T. and A. J. Bowen. 1976. Finite amplitude edge waves. J. Mar. Res. 34(1): 269-293.

6. Guza, R. T. and E. B. Thornton. 1980. Local and shoaled comparisons of sea surface elevations, pressures, and velocities. J. Geophys. Res. 85(C3): 1526-1530.

7. Huntley, D. A. and A. J. Bowen. 1975. Comparison of the hydrodynamics of steep and shallow beaches. In: Nearshore Sediment Dynamics and Sedimentation--an Interdisciplinary Review (eds. J. Hails and A. Carr). John Wiley & Sons, New York.

8. Johns, B. 1980. The modeling of the approach of bores to a shoreline. Coastal Engineeirng 3: 207-219.

9. Komar, P. D. 1977. Beach Processes and Sedimentation. Prentice-Hall, New Jersey, 429 p.

10. Komar, P.D. 1983. Nearshore currents and sand transport on beaches. In: Coastal and Shelf Dynamical Processes, B. Johns [ed.], Elsevier Press.

11. Kumaya, M. and H. Nishimura. 1980. Variation of suspended sediment with wave energy. Proc. 27th Japanese Conf. Coastal Eng., pp. 235-239.

12. Longuet-Higgins, M.S. 1953. Mass transport in water waves. Phil. Trans. Roy. Soc. (London), Series A, 245(903): pp. 535-581.

13. Nielsen, P. 1979. Some basic concepts of wave sediment transport. Series Paper 20, Inst. of Hydrodynamics and Hydraulic Eng., Tech. Univ. of Denmark, Lyngby, 160 p.

14. Phipps, J. B. and J. M. Smith. 1978. Pacific Ocean Beach Erosion and Accretion. State of Washington Dept. of Ecology Unpublished Report, 75 p.

15. Plopper, C. S. 1978. Hydraulic sorting and longshore transport of beach sand, Pacific coast of Washington. Ph.D. thesis, Syracuse Univ., 185 p.

16. Russell, R. C. H. and J. D. C. Osorio. 1958. An experimental investigation of drift profiles in a closed channel. Proc. 6th Coastal Eng. Conf., ASCE, pp. 171-193.

17. U.S. Army Coastal Engineering Research Center. 1977. Shore Protection Manual.

18. U.S. Army Corps of Engineers--Seattle District. 1973. Grays Harbor and Chehalis River and Hoh River, Washington North Jetty Rehabilitation. Unpublished report.

19. Wright, L. D., J. Chappell, B. G. Thom, M. P. Bradshaw, and P. Cowell. 1979. Morphodynamics of reflective and dissipative beach and inshore systems: southeastern Australia. Mar. Geol. 32(1/2): pp. 105-140.

20. Wright, L. D., R. T. Guza and A. D. Short. 1982. Dynamics of a high-energy dissipative surf zone. Mar. Geol. 32: pp. 105-140.

21. Wright, L. D., P. Nielsen, A. D. Short, F. C. Coffey and M. O. Green. 1982. Nearshore and surf zone morphodynamics of a storm wave environment. Eastern Bass Strait, Australia, Coastal Studies Unit, Univ. of Sydney Tech. Rep. No. 82/3, 153 p.